Structural investigation of californium under pressure

S. Heathman[1], T. Le Bihan[2], S. Yagoubi[1,5], B. Johansson[3,4] and R. Ahuja[3,4]

[1] European Commission, Joint Research Center, Institute for Transuranium Elements, Postfach 2340, D-76125 Karlsruhe, Germany
[2] European Synchrotron Radiation Facility – 38043 Grenoble, France
[3] Division of Materials Theory, Department of Physics and Materials Science, Uppsala University, P.O. Box 516, SE-75120 Uppsala, Sweden
[4] Applied Materials Physics, Department of Materials Science and Engineering, Royal Institute of Technology (KTH), SE-100 44 Stockholm
[5] Groupe de Radiochimie, Institut de Physique Nucléaire d'Orsay UMR 8608, Université de Paris-Sud-11, Bât. 100, 91406 Orsay, France

The high pressure structural behaviour of californium has been studied experimentally and theoretically up to 100 GPa. A valence change from divalent to trivalent forms was observed under modest pressure revealing californium to be the only actinide to exhibit more than one metallic valence at near to ambient conditions as is the case for cerium in the lanthanide series. 3 metallic valencies and 4 different crystallographic phases were observed in californium as a function of pressure. High-pressure techniques, synchrotron radiation and *ab initio* electronic structure calculations of total energies were used to investigate the material and to determine the role which californiums 5f electrons play in influencing these transitions. The crystallographic structures observed are similar to those found in the preceding actinide elements, curium and americium with the initially localized 5*f* states becoming completely delocalized under the influence of high pressure.

Introduction

   The transplutonium elements all have localized (non-bonding) 5*f* electrons at ambient pressure which however can participate in bonding at high pressures [1--3]. Previous studies on these elements from americium [4,5] to curium [6] have shown a remarkable diversity of crystallographic structures which appear under pressure due to the influence of this 5*f* electron participation. Atomic volumes are also affected by 5*f* electron bonding across the actinide series with smaller volumes observed in the Pa to Pu metals which result from additional 5*f* bonding already being present at ambient pressure. The pivotal point in the series occurs between plutonium and americium with a sudden increase in atomic volume arising from the transition from itinerant to localized 5*f* states.

In the case of americium [4] we earlier found four crystal structures existing between ambient pressure and 100 GPa with the delocalization of the 5*f* electrons occurring in two stages. The 3rd and 4th low-symmetry structures formed at high pressure were a face-centered orthorhombic (Am III) and a primitive orthorhombic structure, (Am IV), with each transition accompanied by an abrupt decrease in the relative atomic volume. The formation of the Am IV structure (space group, *Pnma*), its stability at very high pressures and its subsequently discovered or theorized [7,8] presence in neighboring actinides has established it as an important actinide high-pressure structure supported by theoretical calculations on the structural behaviour of the higher actinides [9--13]. However recent resonant x-ray emission spectroscopy and x-ray absorption near-edge structure experiments [14] and theory [15] on Am have not substantiated the hypothesis of strong mixing of 5*f* states with the valence band and show that the general behavior of actinide 5*f* electrons under compression is not yet fully understood.

In the case of curium [6] an additional monoclinic (Cm III) high pressure phase was discovered between 37 and 56 GPa which was found to be stabilized by the spin polarization of curiums 5*f* electrons. Subsequent investigations into the high pressure behavior of curium-berkelium

1

alloys [16] as well as previous studies on americium-curium alloys [17] have shown the Cm III phase to be unique in the sense that dilution of curium with its near neighbors is sufficient to prevent its formation. The $5f^7$ electronic configuration of the Cm III phase necessary to maximize magnetic spin polarization is clearly de-stabilized by alloying with adjacent neighboring actinides.

As a result of decreasing half-lives and available quantities of the successively heavier transplutonium elements, californium is at present the heaviest actinide on which structural studies can be performed. The intent of this present study was to perform the first synchrotron radiation investigation of californium up to 100 GPa in order to understand correctly its structural behavior under pressure.

Experimental.

Foils of californium (^{249}Cf isotope ($t_{1/2}$ = 350.6 yr)) metal were prepared at Oak Ridge National Laboratory (ORNL) by vacuum vapor deposition after reduction of its oxide with lanthanum metal [18,19]. Diamond anvil cells are widely used for studying microgram quantities of materials up to and beyond the megabar range. In our experiments both Syassen-Holzapfel (up to 60 GPa) and Cornell-Type (up to 100 GPa) pressure cells were used with diamond culets of between 100 and 300 μm depending on the pressure range studied. Gasket materials used were Inconel and T301 steel with holes of 50 to 150 μm, again depending on the pressure range studied. Four separate series of experiments were performed over a period of 5 years at the European Synchrotron Radiation Facility (ESRF) ID27 and ID30 beam lines in the angular dispersive mode using a monochromatic beam of either 33.17 keV (0.3738 Å), 46.83 keV (0.26472 Å) or 61.33 keV (0.2022 Å). For each experiment 4 to 6 Cf microsamples were loaded together with pressure transmitting medium (liquid N_2 or silicone oil) and pressure gauges (ruby crystal, Cu or Pt powder). Due to the high specific activity of ^{249}Cf only samples of 1 μg or less per pressure cell were allowed at the synchrotron beam line

which presented a particularly difficult technical challenge compared to other actinides previously studied. Technical details about loading actinide samples and the radioactive containment required for synchrotron experiments can be found here [20]. Diffraction images were captured with a Bruker 6500 charge coupled device (CCD) detector or MAR 345 and 165 image plate detectors. The diffraction images were then processed using the ESRF Fit2D program [21] and the fully integrated profiles were refined with the FULLPROF Rietveld analysis program [22].

Theory.

In order to study the electronic structure of Cf, we have used the full-potential linear muffin-tin-orbital (FPLMTO) method [23,24]. The calculations were based on the generalised gradient approximation and we used the Perdew and Wang parameterisation for the exchange and correlation potential. The spin-orbit coupling was included explicitly. Basis functions, electron densities, and potentials were calculated without any geometrical approximation. These quantities were expanded in combinations of spherical harmonic functions (with a cut-off $l_{max} = 6$) inside non-overlapping spheres surrounding the atomic sites (muffin-tin spheres) and in a Fourier series in the interstitial region. The muffin-tin sphere occupied approximately 80% of the unit cell. The radial basis functions within the muffin-tin spheres are linear combinations of radial wave functions and their energy derivatives, computed at energies appropriate to their site and principal as well as orbital atomic quantum numbers, whereas outside the muffin-tin spheres the basis functions are combinations of Neuman or Hankel functions. In the calculations reported here, we made use of pseudo-core $6s$, $6p$ and valence band $7s$, $7p$, $6d$ and $5f$ basis functions with corresponding two sets of energy parameters, one appropriate for the semi-core $6s$ and $6p$ states, and the other appropriate for the valence states. The resulting basis formed a single, fully hybridising basis set. This approach has previously proven to give a well converged basis. For sampling the irreducible wedge of the Brillouin-

zone we used the special k-point method. In order to speed up the convergence, we have associated each calculated eigenvalue with a Gaussian broadening of width 20 mRy.

Valence.

Depending on the preparation technique used, californium is known to exhibit face-centered cubic, double hexagonal close packed or possible hexagonal close packed phases [18,19,25--30] as shown in Table 1 but only the dhcp and fcc structures have been observed in subsequent high pressure experimental work. Differing lattice parameters may be interpreted as divalent, intermediate valence and trivalent forms as shown in Tables 2.

As a result of this coexistence in the bulk sample of 2 metallic valences and probable intermediate valence, the Cf system is considerably more complicated than the Am, Cm and Bk systems.

Figure 1 shows the crystal promotion energies [31] across the actinide series with the bar representing an estimate of the energy required to promote an electron from the f to d level where it can be seen that californium falls into the border region between divalent and trivalent metallic bonding. Further evidence of this borderline state for Cf is that whereas the preceding actinides from Am to Bk usually form trivalent compounds, californium exists in a divalent ionic state [32,33] as well as trivalent.

Theoretical calculations [1,34,35] have predicted a stable metallic divalent state for californium's neighbor einsteinium but only possible surface divalency for californium suggesting a metastable divalent state may exist for Cf depending on the preparation method used and whether the sample takes the form of a thin film or is bulk material. A similar situation exists for the lanthanide samarium which has been found to exhibit divalency in thin films [36] whereas its neighbor europium is divalent in bulk form. This possibility of a divalent surface on top of a bulk trivalent metal was first proposed in refs [31,37].

4

The only lanthanide thought to exhibit a possible valence change under pressure is cerium [38], and many theories have been advanced to elucidate this phenomenon [39-45].

Valency is defined as the number of electrons in the occupied part of the valence band which participate in the conduction and bonding. For cerium this means a change in the behaviour of the 4f electron or if the 4f state remains localized (non-bonding) there must be a change in the 4f occupancy in order to have a change in valency. For cerium the 15% collapse in its atomic volume which occurs under a relatively small pressure is consequently mainly attributed to an interaction between its 4f and conduction electrons. The question of cerium's valency is still a matter of controversy and some experiments suggest that its valency does not necessarily change by 1 electron as was originally expected in the earlier papers on the volume collapse. Some authors suggest intermediate valencies between the trivalent and tetravalent states [46,47]. Recent experiments also propose that the f electronic structure of cerium is governed as much by the sequence of crystallographic stacking as by interaction with its valence d electrons [48]. In the case of californium we observed both divalent and intermediate valent forms of the metal which transformed rapidly under pressure to the trivalent form.

Due to the safety issues associated with these samples, all the pressure cells studied at the ESRF had some starting pressure applied to ensure the containment of the material. This varied from 0.1 to 1 GPa for cells loaded with silicone oil as PTM and between 2 and 3 GPa for samples loaded with nitrogen. Consequently samples containing various mixed valent states were observed in different cells depending on the starting pressure and these lattice parameters are given in Table 2. Ambient pressure laboratory x-ray examination of microgram thin foils of the samples at ITU Karlsruhe gave lattice parameters of a = 5.426 Å for the divalent form, 5.223 Å for the intermediate form and 4.783 Å (fcc), a=3.380 Å c=11.025 Å (dhcp) for the trivalent form. At ambient pressure the divalent californium represented approximately 10% of the total sample with the rest being trivalent which is

5

consistent with this being a surface phenomenon as bulk samples appear to show predominantly the trivalent form. One previously proposed divalent form of Cf shown in Table 1 with (hexagonal a=3.988 Å c=6.887 Å) and (fcc a=5.743 Å) structures was never observed in our studies or identified in other preparations from Table 1. Zachariasen [49] showed that these two forms could not be pure Cf and identified them most likely to be Cf_2O_2S and CfS compounds.

Figures 2a and 2b show the transitions observed between divalent and intermediate valency Cf to the trivalent form. Both divalent and intermediate forms transformed completely to the trivalent form by 4 GPa.

High Pressure Results.

Previous results with californium were obtained at lower pressures than here [50,51].

Not taking into account the divalent - intermediate - trivalent transitions all samples of Cf studied presented a mixture of double hexagonal close packed (dhcp $P6_3$/mmc; Cf I) and face centered cubic (fcc Fm3m; Cf II) phases at low pressure with traces of CfN impurity in 2 of the samples studied [Figure 2].

An example diffraction image of the highly radioactive Cf sample at low pressure can be seen in Fig. 3 with the actual loading configuration enhanced in the figure insert. Some of the unusual diffraction spot effects may be due to macroscopic clusters of crystal defects caused by radiation damage in the crystal lattice as these were not noticeable immediately after sample preparation. Due to this time related problem of radiation damage occurring, great care was taken to perform the synchrotron experiments as soon as possible after sample preparation although the complexities of transporting highly radioactive material between ORNL and ESRF meant that a minimum of 4 weeks passed between preparation and experiment. We found that these possible cluster defects observed at low pressure are

completely removed after the samples underwent structural phase changes at high pressure due to pressure annealing.

With the application of pressure, the dhcp/fcc mixture of Cf I & II phases gradually converts to the pure fcc structure Cf II which is completed at about 14 GPa [Figure 4].

With additional pressure, the Cf II phase converts to a very complex spectrum at above 35 GPa which is retained up to 100 GPa [Figure 5]. The structure of this high pressure phase was determined to comprise of a mixture of 2 orthorhombic phases previously identified in our study on americium [4], namely: Am III and Am IV. The Cf III structure (isostructural with Am III) has a face-centered orthorhombic cell (space group Fddd, Cf on the 8a sites, all position parameters fixed by symmetry) and was observed between 38 and 100 GPa. The Cf IV structure (isostructural with Am IV) has a base-centered orthorhombic structure (Pnma, primitive orthorhombic) and was also observed between 38 and 100 GPa. This unexpected 2 phase existence over a large pressure range is discussed in more detail later.

In one experiment a Cf sample experienced a sudden rapid pressure increase from about 30 to 95 GPa due to the sudden release of a blocked piston in a Cornell pressure cell. The final pressure after relaxation stabilized at 80 GPa and in this unique case we obtained a pure spectrum of the Cf III phase shown in Fig. 6 which was retained in its pure form whilst further releasing pressure. This was the only time that a pure Cf III phase predicted by theory to be energetically more stable at very high pressure was observed without the presence of the Cf IV phase. Retransformation to the pure fcc Cf II phase was completed by 26 GPa.

Volume and bulk modulus.

A plot of the relative volumes (V/V_o, where V_o is the volume at atmospheric pressure) versus pressure is given in Fig. 7 showing the different structural regions and the relative volume changes. Abrupt volume collapses of 4.8% at the Cf II to Cf III transition, and 10% between the Cf III and Cf IV phases are observed. These are larger than the 2% and 7%

collapses observed in Am, but very similar to the 4.5% and 11.7% values found in Cm where in that case the first collapse is between the Cm II fcc phase and the Cm III monoclinic phase. As was the case for Am and Cm we believe that these two volume collapses should both be attributed to f electron delocalization processes and represent a stepwise delocalization process. This idea of gradual delocalization occurring across the Fddd to Pnma transitions in the heavy actinides is strengthened by resistivity studies of Am under pressure [52] which also indicate that the $5f$ electrons are not fully delocalized until the onset of the Am IV phase. Resistivity studies on Pu/Am alloys [53] have attributed this to $5f^6$-$5f^7$ valence fluctuations rather than a simple delocalization. In the inset of Fig. 7, we have shown our calculated Energy vs volume plot. Here, we have not shown the dhcp phase as we are interested in the high pressure behavior of Cf. Our calculations show structural transformations from Cf-II (fcc) to Cf-III (Fddd) to Cf-bcc. Our calculations do not show a stability of the Cf-IV (Pnma) phase which is different from the case of Am or Cm. Nevertheless it can be seen that the energy difference between the Cf-III and Cf-IV structures is relatively small in this case. Our calculations predict that the bcc phase becomes stable at very high pressure which at present cannot be confirmed experimentally as it is above the attainable pressure range.

The compressibility for Cf was obtained by fitting the Birch - Murnaghan [54] and Vinet [55] equations of state to the low pressure phases (regions of localized f electrons) to obtain the bulk modulus B_0 and its pressure derivative B'_0. Both calculations gave similar values, which were 36.2(3) GPa for B_0 and 3.9(2) for B'_0 and 35.3(3) GPa for B_0 and 4.3(3) for B'_0, respectively. The theoretical bulk modulus was calculated to be 36.7 GPa and 4.0 for B'0, in excellent agreement with the experimental results. These californium moduli are in line with values for the pure Am-Cf metals, which range from 25 to 43 GPa but considerably smaller than the moduli of the Th - Pu metals, which have additional bonding from their itinerant f electrons and are less compressible.

CfN.

The presence of approximately 5-10 % CfN (a_0= 4.983 Å) [56,57] in some of the measured samples enabled us to follow the progression of its compressibility alongside that of the pure Cf metal. It should be noted that the few samples containing CfN impurities were only used to follow the CfN compressibility and not used to identify the Cf III and IV structures. The fcc structure of CfN remains stable up to 44 GPa, the highest pressure at which we were able to quantifiably determine peak positions before the advent of the complex spectra resulting from the appearance of the Cf III and Cf IV structures. We determined a bulk modulus for CfN of Bo= 122.0 GPa and Bo'= 5.4.

Conclusions.

Our high pressure study of californium has revealed the presence of three metallic valence states depending on the sample preparation methods used and whether the material is a thin film or bulk sample. Divalent and intermediate valent forms of Cf were observed which all transformed under moderate pressure to the trivalent form confirming that a metastable divalent state exists for Cf as suggested from the calculation of crystal promotion energies required to promote an electron from the *f* to *d* level [31,58] . Cf therefore clearly falls into the border region between divalent and trivalent metallic bonding which is a phenomenon only previously observed in the lanthanide Sm.

Given the complexity of sample preparation, purification and handling for Cf it is important to note that small quantities of La metal used in the reduction of the initial Cf oxide may have formed in its high temperature fcc form on the surface of the prepared material. If this were the case we would expect a lattice parameter of about 5.2 Å which corresponds to the observed lattice parameter attributed to intermediate valence Cf. In addition surface layers of complex oxides between $CfO_{1.5-2.0}$ may have formed with fcc lattice parameters close to

those reported here for divalent Cf of around 5.4 Å. The problem here is that under greater

pressure the samples all showed either the pure Cf fcc phase [Figure 4] or in one case the pure

Fddd phase [Figure 6] without any significant trace of other phases. If a coating of La metal

or Cf oxide was on the surface, it would therefore have to "disappear" into the bulk of the

product at higher pressure and not be readily seen. To the authors knowledge such behaviour

has not been observed or confirmed in other high pressure experiments in which a strongly

diffracting oxide layer is completely absorbed into the bulk material under pressure.

A thin layer of La metal could potentially be pressed into forming an alloy with Cf but would

be unlikely at RT. Under pressure lanthanum metal would be expected to adopt the distorted

fcc structure between 7 and 60 GPa [59] whereas Cf retains the simple fcc structure until 35

GPa. Diffraction lines corresponding to an impurity dist-fcc phase would be expected if La

were present in this pressure range. However the corresponding diffraction lines of a dist-fcc

phase were not observed in the simple spectra of pure Cf fcc in the pressure range between 14

and 35 GPa where they should be clearly resolved. Another argument in this particular case

against absorption of an impurity surface layer into the bulk sample concerns those

experiments reported in this paper where we have observed clearly defined CfN diffraction

peaks corresponding to the cubic phase which were well resolved and constant in intensity

from ambient pressure up to 44 GPa regardless of the phase changes occurring in the bulk Cf

material.

Under pressure Cf follows the same sequence of structural phase transitions as the preceding

actinides Am and Cm except that the unique Cm III phase is not formed and a co-existence of

the 2 "collapsed" orthorhombic phases Cf III and Cf IV is observed above 38 GPa.

The present theory shows that the energies required for the stabilization of these 2 structures

are very similar at the transition from the fcc phase and that the Cf III Fddd phase should be

preferred at higher pressure. In the 2006 theory paper by Per Söderlind [13] Figure 11 shows

identical energies for both Cf III Fddd and Cf IV Pnma phases at 50 GPa with the Fddd phase becoming more stable above this pressure. This earlier theory result seems to fit the experimental data particularly well and explains our observation of the pure Fddd phase above 80 GPa. Non hydrostatic sample conditions in different regions of the gasket hole above 50 GPa may be a partial explanation for the retention of both phases except in the case of Figure 6 where a sudden shock rapid increase of pressure stabilized the pure Fddd phase as predicted by theory. Although unusual, the retention of 2 phases with differing volumes over a large pressure range has been observed previously in the case of cerium metal [60]. Here the alpha and gamma phases were found to co-exist with a 14% volume difference between them, which is even greater than the 10% observed between Cf III and Cf IV. For Ce the mechanism of co-existence is explained as a diffusionless first order transition induced by dislocation motion or strain energy. In the case of californium the transition is not isomorphic but a similar mechanism may be applicable in justifying the co-existence of the Cf III and Cf IV phases. Essentially the theory tells us that the Fddd and Pnma structures are in equilibrium despite their different volumes and their stabilization will depend on the exact pressure conditions and corresponding intergranular strains.

Stepwise volume collapses of 4.8% and 10% were observed across the transition from localized to fully de-localized states similar to those previously observed in Cm. An average experimental bulk modulus of 35.8(5) GPa was determined for Cf which is in good agreement with the calculated theoretical value also presented in this paper of 37.4 GPa.

Acknowledgements.

Table 1.

Crystallographic data previously reported for californium

Crystal System	Lattice a_0 (Å)	Parameters c_0 (Å)	Atomic Volume (Å³/atom)	Crystal Density (g cm⁻³)	Metallic Radius (Å)	Ref
hcp	3.988	6.887	47.4	8.72	2.07	[18]
fcc	5.743		47.4	8.72	2.03	[18]
dhcp	4.002	12.804	44.4	9.31	1.99	[19]
fcc	5.40		39.4	10.5	1.91	[18,25,26]
fcc	4.994		30.1	13.7	1.75	[27]
fcc	4.94		30.1	13.7	1.75	[28,29]
dhcp	3.38	11.025	27.3	15.2	1.69	[26,61]
dhcp	3.39	11.01	27.4	15.1	1.69	[28]
fcc	4.78		27.4	15.1	1.69	[56]
dhcp	3.384	11.040	27.4	15.1	1.69	[19,30]
fcc (CfN)	4.94		30.1	13.7	-	[56]

References: [18] Haire & Baybarz (1974), [19] Haire & Asprey (1976), [25] Cunningham & Parsons (1970), [26] Radchenko *et al.* (1986), [27] Stevenson (1973), [28] Noé & Peterson (1976), [29] Burns & Peterson (1978), [61] Seleznev *et al.* (1989), [30] Seleznev *et al.* (1990), [56] Haire *et al.* (1986)

Table 2.

Experimental lattice parameters for Cf from ESRF high pressure experiments

Phases Observed	Sample 1 *(0.4GPa)*	Sample 2	Sample 3 *(3GPa)*	Sample 4 *(0.1GPa)*
dhcp (Cf I) trivalent	a = 3.38 Å c = 11.02 Å	a = 3.38 Å c = 11.025 Å	a = 3.29 Å c = 10.75 Å	a = 3.404 Å c = 11.157 Å
fcc 1 (Cf II) trivalent	a = 4.771 (Å)	a = 4.783 (Å)	a = 4.64 (Å)	a = 4.783 (Å)
fcc 2 Cf intermed.	a=5.215 Å	----	a = 5.136 (Å)	a = 5.2232 Å
fcc 3 Cf divalent	----	a = 5.426 Å	a = 5.340 Å	----
fcc (CfN)	----	a = 4.983 (Å)	a = 4.92 (Å)	----

Figure Captions.

Figure 1. Divalent - Trivalent zones for actinides and lanthanides [31,58]

Figure 2a. Transitions between divalent and intermediate valency Cf to the trivalent form.

Wavelength 0.26472 Å

Figure 2b. Intermediate valent Cf (a=5.2232 Å) to trivalent transition between 0.1 and 3.8 GPa. Wavelength 0.3738 Å

Figure 3. Diffraction image of ~1 µg Cf at 3 GPa. Insert shows cell loading.

Figure 4. Rietveld fit of the fcc (space group *Fm 3m*) pure trivalent Cf II phase at 20 GPa (wavelength = 0.2022 Å, pressure transmitting medium nitrogen) showing calculated reflection tick marks, Miller indices, principal reflections and difference profile.

Figure 5. Rietveld fit of orthorhombic (space groups Fddd and Pnma) Californium phases III and IV at 100 GPa showing calculated reflection tick marks, principal reflections and difference profile. Cu indicates copper pressure marker peaks. Fddd a = 8.453, b = 4.891, c = 2.605 Å, Bragg-R Factor=3.84%, Pnma a = 4.792, b = 3.777, c = 2.695 Å, Bragg-R Factor=2.92%. Wavelength 0.3738 Å.

Figure 6. Rietveld fit of orthorhombic (space group Fddd) Californium phase IV at 80 GPa (decreasing pressure) showing calculated reflection tick marks, principal reflections and difference profile. Wavelength 0.3738 Å.

Figure 7. Relative volume-versus-pressure-curve for californium + theory.

References.

1 B. Johansson, Physical Review B **11**, 2740 (1975).

2 H. L. Skriver, O. K. Andersen, and B. Johansson, Phys. Rev. Lett. **41**, 42 (1978).

3 H. L. Skriver, O. K. Andersen, and B. Johansson, Phys. Rev. Lett. **44**, 1230 (1980).

4 S. Heathman, R. G. Haire, T. Le Bihan, A. Lindbaum, K. Litfin, Y. Méresse, and H. Libotte, Physical Review Letters **85**, 2961 (2000).

5 A. Lindbaum, S. Heathman, K. Litfin, Y. Méresse, R. G. Haire, T. Le Bihan, and H. Libotte, Phys.Rev.B **63**, 214101 (2001).

6 S. Heathman, R. G. Haire, T. Le Bihan, A. Lindbaum, M. Idiri, P. Normile, S. Li, R. Ahuja, B. Johansson, and G. H. Lander, Science **309**, 110 (2005).

7 P. Söderlind, R. Ahuja, O. Eriksson, B. Johansson, and J. M. Wills, Physical Review B **61**, 8119 (2000).

8 M. Pénicaud, Journal of Physics Condensed Matter **14**, 3575 (2002).

9 M. Pénicaud, Journal of Physics Condensed Matter **17**, 257 (2005).

10 M. Pénicaud, MRS Online Proceedings Library **893** (2005).

11 A. Landa, P. Söderlind, A. Ruban, L. Vitos, and L. Pourovskii, Phys.Rev.B **70**, 224210 (2004).

12 P. Söderlind and A. Landa, Physical Review B - Condensed Matter and Materials Physics **72**, 024109 (2005).

13 P. Söderlind, MRS Online Proceedings Library **893** (2005).

14 S. Heathman, J. P. Rueff, L. Simonelli, M. A. Denecke, J. C. Griveau, R. Caciuffo, and G. H. Lander, Phys.Rev.B **82**, 201103 (2010).

15 P. Söderlind, K. T. Moore, A. Landa, B. Sadigh, and J. A. Bradley, Phys.Rev.B **84**, 075138 (2011).

16 S. Heathman, R. G. Haire, T. Le Bihan, R. Ahuja, S. Li, W. Luo, and B. Johansson, Journal of Alloys and Compounds **444-445**, 138 (2007).

17 T. Le Bihan, R. G. Haire, S. Heathman, M. Idiri, and A. Lindbaum, Journal of Nuclear Science and Technology **3**, 45 (2002).

18 R. G. Haire and R. D. Baybarz, Journal of Inorganic and Nuclear Chemistry **36**, 1295 (1974).

19 R. G. Haire and L. B. Asprey, Inorganic and Nuclear Chemistry Letters **12**, 73 (1976).

20 R. G. Haire, S. Heathman, T. Le Bihan, and A. Lindbaum, NEA Publication, ISBN 92-64-18485-6, 147 (2002).

21 A. P. Hammersley, S. O. Svensson, M. Hanfland, A. N. Fitch, and D. Hausermann, High Pressure Research **14**, 235 (1996).

22 J. Rodríguez-Carvajal, Physica B: Condensed Matter **192**, 55 (1993).

23 J. M. Wills and B. R. Cooper, Phys.Rev.B **36**, 3809 (1987).

24 D. L. Price and B. R. Cooper, Phys.Rev.B **39**, 4945 (1989).

25 B. B. Cunningham and T. C. Parsons, Nucl. Chem. Ann. Rept. Univ. of Calif., UCRL-20426 (1970).

26 V. M. Radchenko, A. G. Seleznev, and R. R. Droznik, Sov. Radiochem. **28**, 401 (1986).

27 J. N. Stevenson, *ORO-4447-004 (TID-26453)* (University of Tennessee, Knoxville, 1973).

28 M. Noé and J. R. Peterson, *Preparation and Study of Elemental Californium-249*, edited by W. Müller and R. Lindner (North-Holland Publishing Co, Amsterdam, 1976), p. 69.

29 J. H. Burns and J. R. Peterson, Inst Phys Conf Ser **37**, 52 (1978).

30 A. Seleznev, V. Radchenko, V. Shushakov, M. Ryabinin, R. Droznik, L. Lebedeva, and V. Vasilyev, J. Radioanal. Nucl. **143**, 253 (1990).

31 B. Johansson, Phys.Rev.B **19**, 6615 (1979).

32 J. R. Peterson and R. D. Baybarz, Inorganic and Nuclear Chemistry Letters **8**, 423 (1972).

33 H. A. Friedman, J. R. Stokely, and R. D. Baybarz, Inorganic and Nuclear Chemistry Letters **8**, 433 (1972).

34 M. S. S. Brooks, B. Johansson, and H. L. Skriver, *Handbook on the Physics and Chemistry of the Actinides*, edited by A. J. Freeman and G. H. Lander (North Holland, Amsterdam, 1984), 1, p. Chap. 3, p. 153-269.

35 B. Johansson and A. Rosengren, Physical Review B **11**, 1367 (1975).

36 J. W. Allen, L. I. Johansson, R. S. Bauer, I. Lindau, and S. B. M. Hagström, Physical Review Letters **41**, 1499 (1978).

37 B. Johansson, Inst Phys Conf Ser **37**, 39 (1978).

38 W. H. Zachariasen and F. H. Ellinger, Acta Crystallographica Section A **33**, 155 (1977).

39 H. Eckardt and L. Fritsche, Journal of Physics F: Metal Physics **16**, 1731 (1986).

40 B. Johansson, Hyperfine Interactions **128**, 41 (2000).

41 P. Söderlind, O. Eriksson, J. Trygg, B. Johansson, and J. M. Wills, Physical Review B **51**, 4618 (1995).

42 A. Svane, Physical Review B - Condensed Matter and Materials Physics **53**, 4275 (1996).

43 T. Watanabe and A. Sakuma, Physical Review B **31**, 6320 (1985).

44 J. W. Allen and R. M. Martin, Phys. Rev. Lett. **49**, 1106 (1982).

45 B. Johansson, Philosophical Magazine **30**, 469 (1974).

46 K. Held, A. K. McMahan, and R. T. Scalettar, Physical Review Letters **87**, 276404 (2001).

47 J. Röhler, *High energy spectroscopy*, edited by K. A. Gschneidner Jr, L. Eyring and S. Hüfner (Elsevier Science Publ. B.V, Amsterdam, 1987), 10, p. Chap. 71.

48 K. T. Moore, B. W. Chung, S. A. Morton, A. J. Schwartz, J. G. Tobin, S. Lazar, F. D. Tichelaar, H. W. Zandbergen, P. Soderlind, and G. van der Laan, Physical Review B (Condensed Matter and Materials Physics) **69**, 193104 (2004).

49 W. H. Zachariasen, Journal of Inorganic and Nuclear Chemistry **37**, 1441 (1975).

50 U. Benedict, J. R. Peterson, R. G. Haire, and C. Dufour, Journal of Physics F: Metal Physics **14**, L43 (1984).

51 J. R. Peterson, U. Benedict, C. Dufour, I. Birkel, and R. G. Haire, Journal of the Less-Common Metals **93**, 353 (1983).

52 J. C. Griveau, J. Rebizant, G. H. Lander, and G. Kotliar, Phys. Rev. Lett. **94**, 097002 (2005).

53 A. V. Kolomiets, J. C. Griveau, S. Heathman, A. B. Shick, F. Wastin, P. Faure, V. Klosek, C. Genestier, N. Baclet, and L. Havela, EPL (Europhysics Letters) **82**, 57007 (6pp) (2008).

54 F. Birch, Physical Review B **71**, 809 (1947).

55 P. Vinet, J. Ferrante, J. H. Rose, and J. R. Smith, J. Geophys. Res **92**, 9319 (1987).

56 R. G. Haire, U. Benedict, J. R. Peterson, C. Dufour, and S. Dabos, Physica **144B**, 19 (1986).

57 R. Haire, *Californium*, edited by L. Morss, N. Edelstein and J. Fuger (Springer Netherlands, 2006), p. 1499.

58 B. Johansson, Journal of Physics and Chemistry of Solids **39**, 467 (1978).

59 F. Porsch and W. B. Holzapfel, Phys. Rev. Lett. **70**, 4087 (1993).

60 F. Decremps, L. Belhadi, D. L. Farber, K. T. Moore, F. Occelli, M. Gauthier, A. Polian, D. Antonangeli, C. Aracne-Ruddle, and B. Amadon, Phys. Rev. Lett. **106**, 065701 (2011).

61 A. G. Seleznev, V. M. Radchenko, and V. D. Shushakov, Sov. Radiochem. **6**, 637 (1989).
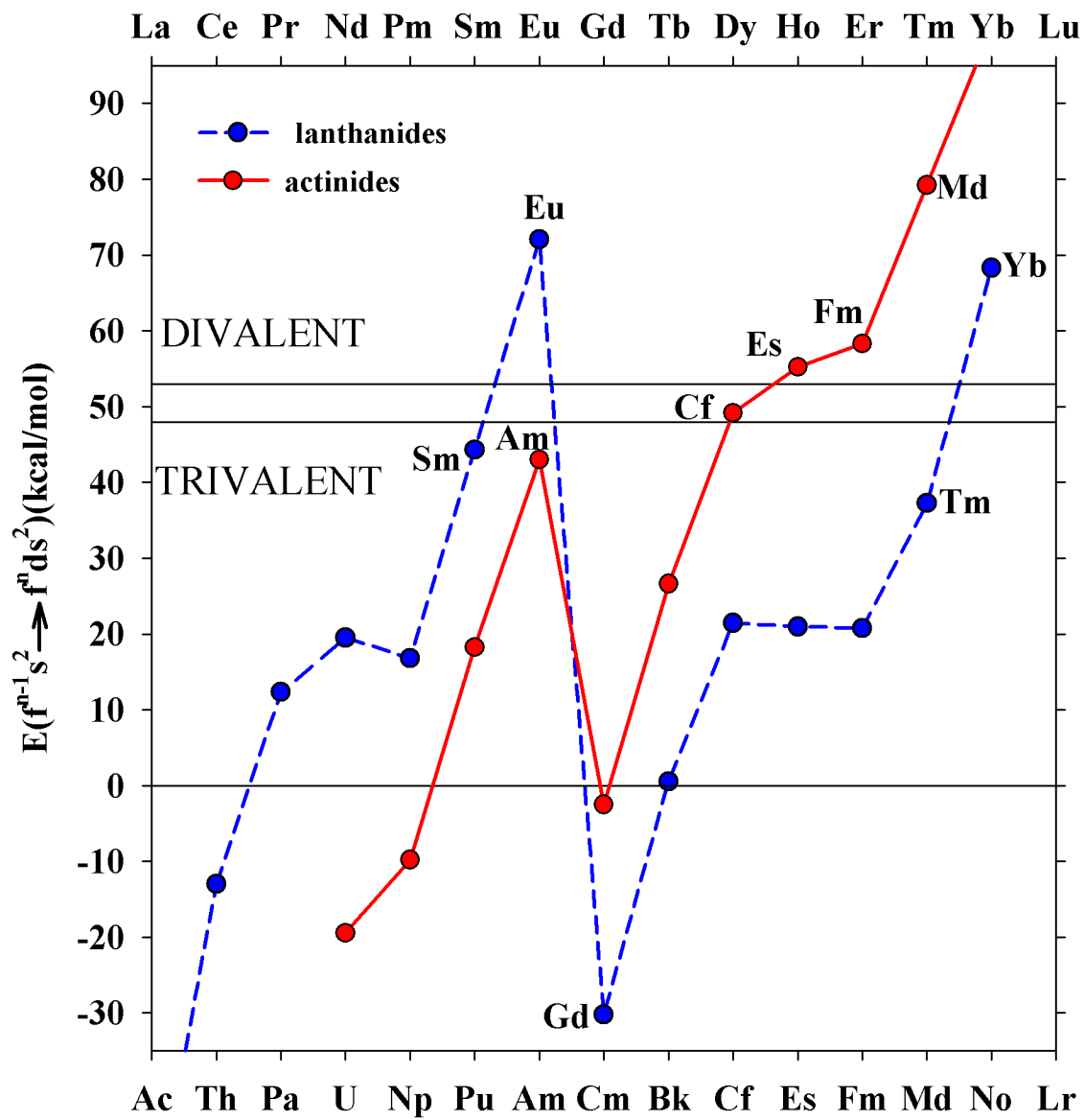
f - d promotion energies for the f-elements

80 μm